Int. J. Electrochem. Sci., 8 **(2013)** 1735 - 1758

International Journal of
ELECTROCHEMICAL
SCIENCE
www.electrochemsci.org

Spectroscopic Characterization of Red Onion Skin Tannin and It's use as Alternative Aluminium Corrosion Inhibitor in Hydrochloric Acid Solutions

N.J.N. Nnaji[1,*], *C.O.B. Okoye*[1], *N.O. Obi-Egbedi*[2], *M.A.Ezeokonkwo*[1] *and J.U.Ani*[1]

[1] Department of Pure and Industrial Chemistry, University of Nigeria, 410001, Nsukka, Enugu State-Nigeria.
[2] Department of Chemistry, University of Ibadan, Ibadan-Nigeria.
[*]E-mail: joemeks4u@yahoo.com

Received: 17 October 2012 / *Accepted:* 16 January 2013 / *Published:* 1 February 2013

Characterization of red onion skin tannin (ROST) was done using FTIR and UV/visible spectrophotometric techniques, revealing ROST to be made up of mixed (hydrolysable and condensed) tannins. ROST has been found to be an effective corrosion inhibitor of aluminium in hydrochloric acid solutions using gravimetric, thermometric, and UV/visible spectrophotometric techniques. Proposed kinetic model reveals complex reaction mechanism (parallel reactions) for aluminium corrosion inhibition by ROST. ROST adsorption on aluminium followed Langmuir isotherm in 0.1M and Fruendlich isotherm in 0.5M HCl and 2.0M HCl at 303 Kelvin. Physical adsorption (physisorption) of ROST on aluminium has been proposed.

Keywords: Aluminium; Weight Loss; Acid Inhibition

1. INTRODUCTION

Tannins are inexpensive agricultural byproducts which have been used extensively for industrial purposes. This is because tannins are non-toxic, hence, environmentally friendly and polyphenolic compounds widely found in nature. Tannins are water soluble, hence, extracting them from leaves, fruits, barks and wood of plants are not difficult. Their industrial applications include: tannantes [1, 2], manufacture of inks [3], antioxidants, food additives, pharmaceuticals and medicine [4-10].

The use of tannin as corrosion inhibitor was necessitated by the recent need to produce environmentally friendly, readily available and economical corrosion inhibitors. The present work therefore aims at characterizing red onion skin tannin (ROST) and investigating its effectiveness as

aluminium corrosion inhibitor in hydrochloric acid solutions. In addition, this present effort would propose a new mechanism for the kinetics of corrosion inhibition of aluminium in hydrochloric acid solutions. This is necessary as the present kinetic model proposes first order kinetics for highly complex inhibition reactions.

2. EXPERIMENTAL METHODS

2.1. Chemicals and apparatus

Pure aluminium was obtained from TOTS Aluminium Nigeria Limited and used in this study. The aluminium sheet was mechanically press cut into 4cm x 5cm coupons and without polishing, was degreased in absolute ethanol, and dried in acetone. The coupons were weighed and stored in a desiccator prior to use in corrosion studies.

All chemicals used were Analar grade purchased from BDH Chemicals Poole, England. Distilled water was obtained from Equipment Maintainance and Service Centre, University of Nigeria, Nsukka.

2.2. Red onion skin tannin (ROST)

Red onion skin was collected from Ibagwa market near Nsukka. The air dried red onion skin was ground and extracted with 70% aqueous acetone and filtered using Buckner funnel and vacuum pump. The dark brown filtrate was allowed over a period of about six weeks to form a light brown solid.

Infrared spectrum of ROST was obtained on Shimadzu FTIR-8400S infrared spectrophotometer using potassium bromide of spectroscopic grade at NARICT, Zaria in Kaduna State, Nigeria.

UV-Visible spectrum of ROST was obtained using JENWAY 6405 spectrophotometer inter-phased with a computer.

2.3. Mass loss measurements

Clean weighed aluminium coupons were placed in 250 mL beakers containing 100 mL of corrodent (0.1M and 0.5M hydrochloric acid solutions) in the presence and absence of the inhibitor (red onion skin tannin ranging from 0.1 – 0.5 g/L). The beakers were placed in a thermostated oven at 30˚C, 40˚C and 50˚C. The coupons were retrieved at 1 hour, 2 hour, 3 hour and 5 hour intervals progressively for 11 hours, scrubbed with bristle brush in distilled water at room temperature, dried in acetone and weighed. The difference in weight of the coupons were taken as weight loss and used to compute the corrosion rate given by

$$C_{corr} = \frac{M_2 - M_1}{At} \qquad (1)$$

where M_2 and M_1 are the masses of the specimen before and after corrosion respectively, A is the area of the coupon and t is the corrosion time.

Inhibition efficiency (IE) was calculated using the following expression:

$$IE = \frac{W_1 - W_o}{W_1} x\,100 \qquad (2)$$

where W_0 and W_1 are the aluminium corrosion rates in the presence and absence of ROST respectively in hydrochloric acid solutions.

Surface coverage (θ) values were calculated using the following expression

$$\theta = \frac{W_1 - W_o}{W_1} \qquad (3)$$

2.4. Thermometric measurements

The apparatus and procedure for the dissolution of aluminum in acid environment used, is as described elsewhere [11]. The apparatus consists essentially of a two necked reaction flask to which a thermometer is fitted. The reaction flask was lagged to prevent heat exchanges to and from the surroundings. Volume of the test solutions were kept at 50 mL.

The initial temperature in all experiments was at room temperature ($30 \pm 2^{\circ}C$). The variation of temperature with time for the dissolution of aluminum in HCl at all concentrations was monitored at two minute intervals with a calibrated thermometer ($O^{o}C$-$100^{\circ}C$) to the nearest $\pm 0.05^{\circ}C$. Immersions were in the absence and presence of the inhibitor at various concentrations (10-50 g/L). This method allowed for the evaluation of the reaction number (RN), defined as:

$$\text{RN } (^{C}/_{\text{min}}) = \frac{T_m - T_i}{t} \qquad (4)$$

where T_m and T_i are maximum and initial temperatures respectively, and t is the time taken to reach the maximum temperature.

The inhibition efficiency (%I) was evaluated from percentage reduction in the reaction number thus [11]:

$$\%I = \frac{RN_0 - RN_i}{RN_0} X100 \qquad (5)$$

where RN_0 is the reaction number in the absence of inhibitors and RN_i is the reaction number in the presence of the inhibitor.

3. RESULTS AND DISCUSSIONS

3.1. Fourier transformed infrared (FTIR) and UV-visible spectroscopic studies

The FTIR spectrum of ROST is shown in Figure 1. The broad peak centered at 3282 cm^{-1} corresponds to aromatic C-H signals with absorbance at about 0.060 and is in excellent agreement with =C-H signals at that wavelength. The peak at 1650 cm^{-1} corresponds to C=O signal. Also, a peak at 1116 cm^{-1} signals the presence of C-O bonds. The spectrum of ROST has a striking signal at 442 cm^{-1} which corresponds to substituted aromatic rings with absorbance of about 0.733 and also reveals the presence of –OH. These observations are in agreement with those of other works [1, 12] and consistent with the bonds that make up the major constituents of ROST namely: quercetin and quercetin-4$^{!}$-glucoside [13] shown in Figure 1.

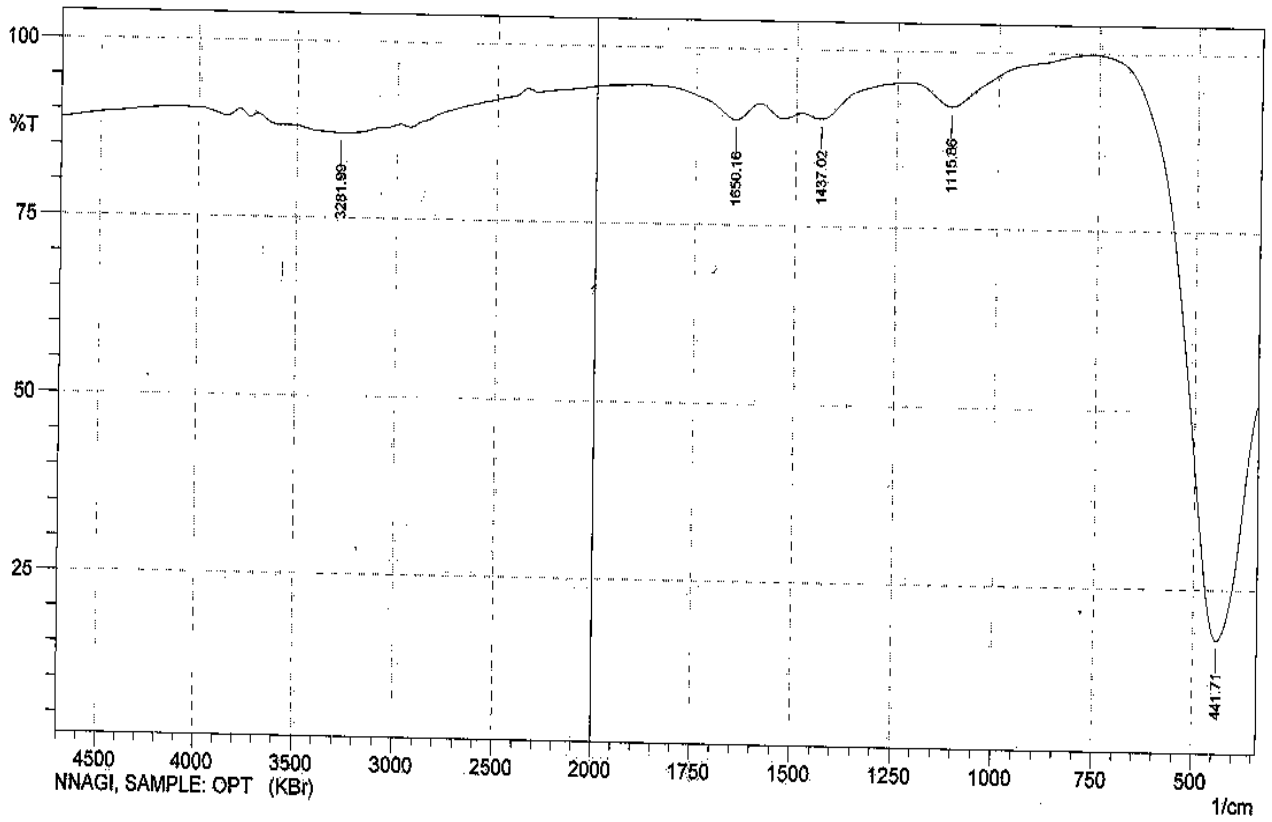

Figure 1. FTIR spectrum of ROST

The UV/visible spectrum of ROST, taken in ethanol, is shown in figure 2. UV/visible spectroscopy is important in determining the nature of vegetable tannins [1, 12]. Figure 2 reveals five peaks ($\lambda_{max_1} - \lambda_{max_5}$) at: 220 nm and 230 nm both with absorbance of 2.162; 255 nm with absorbance of 2.426; 295 nm with absorbance of 1.437; 360 nm with absorbance of 1.942; and 375 nm with absorbance of 1.600.

Applying Woodward-Fieser rules for enone and conjugated diene absorptions on quercetin, shown in figure 3, the following were obtained:

For enone absorption of quercetin:
Parent Value = 215 nm
alpha (OH) = 35 nm
beta (OH) = 30 nm
3 DBE = 90 nm
beta (-O.) = 6 nm
Total = 376 nm

For conjugated diene absorption of quercetin:
Parent Value = 253 nm
DBE = 30 nm
2 OH = 12 nm
Total = 295 nm

Wavelength values calculated from these Woodward-Fieser rules are in excellent agreement with values of 375nm (λ_{max_5}) and 295nm (λ_{max_3}) from UV/visible measurement. With these, we confirm the presence of quercetin in ROST and therefore assign them respectively to (n-π^*) and ($\pi - \pi^*$) transitions respectively. The peaks at $\lambda_{max_1} - \lambda_{max_3}$, are assigned to ($n - \pi^*$) transitions, λ_{max_4} and λ_{max_5} are therefore assigned to ($\pi - \pi^*$) transitions.

Arachis hypogaea tannins were characterized by Ukoha and co-workers [1] using UV-visible spectroscopic method and found two close peaks at 220 nm and 255 nm which they attributed to presence of mixed tannins. On one part, the appearance of the two peaks in the spectrum of ROST therefore suggests it to be composed of mixed (hydrolysable and condensed) tannins.

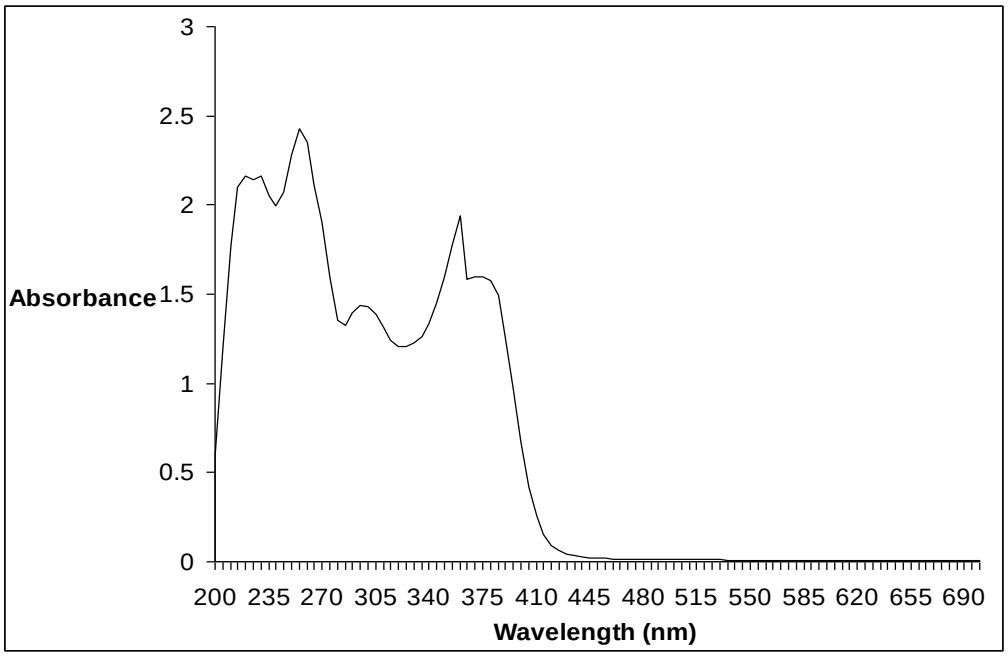

Figure 2. UV/visible spectrum of ROST in ethanol

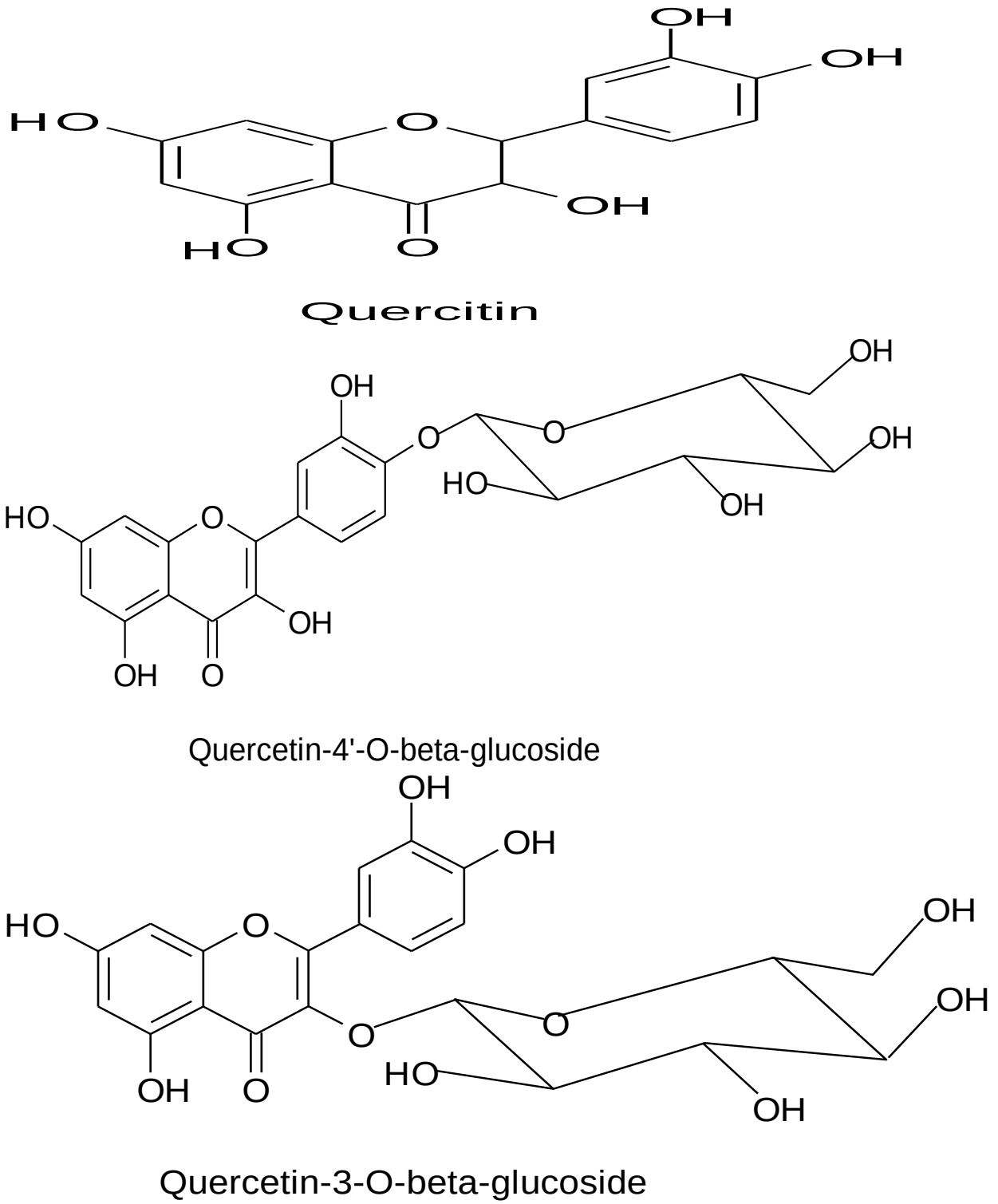

Figure 3. Structures of ROST Components [13]

3.2. Inhibitory action of red onion skin tannin (ROST) on the corrosion of aluminium

The values of inhibition efficiency obtained from gravimetric measurements for various inhibitor concentrations in 0.1M and 0.5M hydrochloric acid at 303Kel-323Kel are shown in Figures 4 and 5. In 0.1M and 0.5M hydrochloric acid solutions, the inhibitor efficiency of ROST generally

increased with increase in inhibitor concentration. However, in 0.5M hydrochloric acid, the inhibition efficiency of ROST decreased when compared to obtained inhibition efficiency values in 0.1M hydrochloric acid solutions. Figures 4 and 5 also reveal that increasing the temperature from 30^0C to 50^0C caused the inhibition efficiency of ROST to decrease. This trend is due to physical absorption of ROST on aluminium such that increase in temperature favours desorption of ROST and results/leads to decreased inhibition. This is in agreement with findings elsewhere [14, 15].

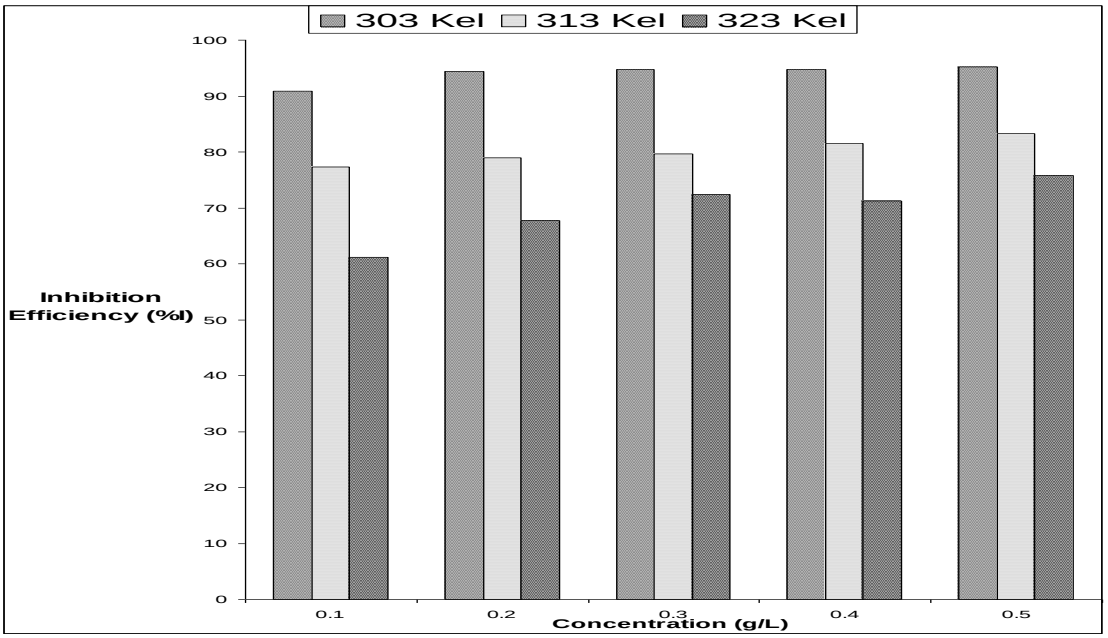

Figure 4. Effect of temperature on inhibition efficiency for various ROST concentrations in 0.1M hydrochloric acid.

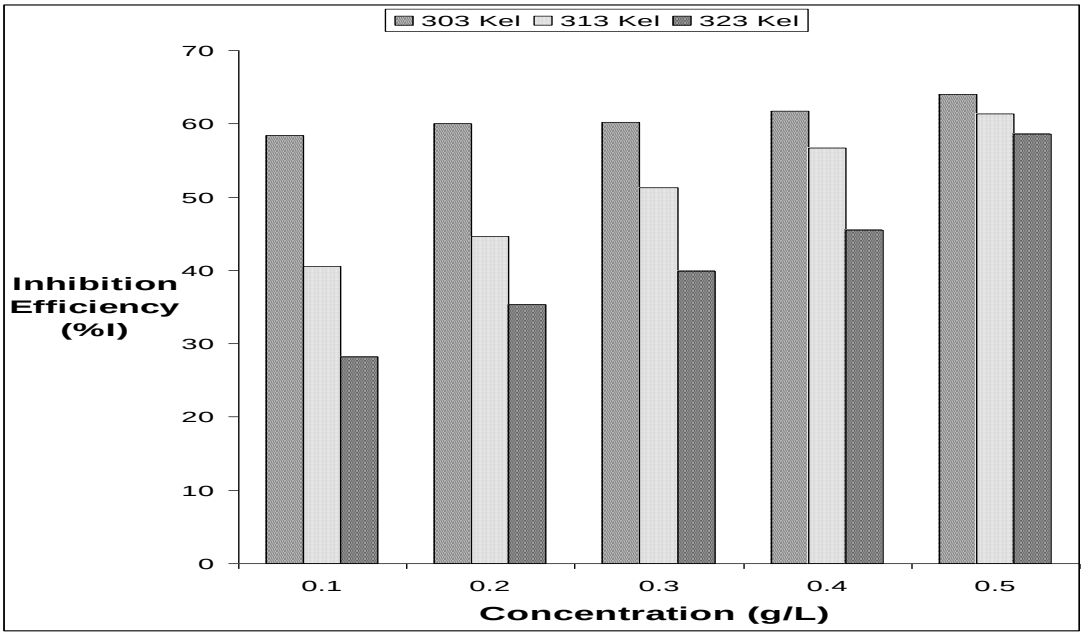

Figure 5. Effect of temperature on inhibition efficiency for various ROST concentrations in 0.5M hydrochloric acid.

A conventional method based on UV/visible absorption spectra gave Figure 6 from 0.1M and 0.5M HCl solutions containing ROST before and after 11 hours of aluminum immersion. Figure 6 reveals four absorptions in the spectra of 0.1 M and 0.5 M HCl solutions containing ROST before aluminium immersion. These absorptions are similar for 0.1M and 0.5M HCl solutions containing ROST before aluminium immersion. After 11 hours, the four absorptions remained unchanged for 0.1M HCl solution, however, the smallest/weakest absorption around 380 nm shifted to around 430 nm for 0.5M HCl solution containing ROST. This is indicative that [ROST-Al^{3+}] complexes formed via π-electron sites of ROST in 0.5M HCl solution. This shift was absent for 0.1M HCl solution containing ROST after 11 hours of aluminium immersion. Its spectrum remained unchanged because corrosion was very minimal in comparison to aluminium corrosion in 0.5 M HCl. These indicate that more aluminium corroded in 0.5M HCl to enable complexation with ROST, hence, explains better aluminium corrosion protection in 0.1M HCl than in 0.5M HCl by ROST.

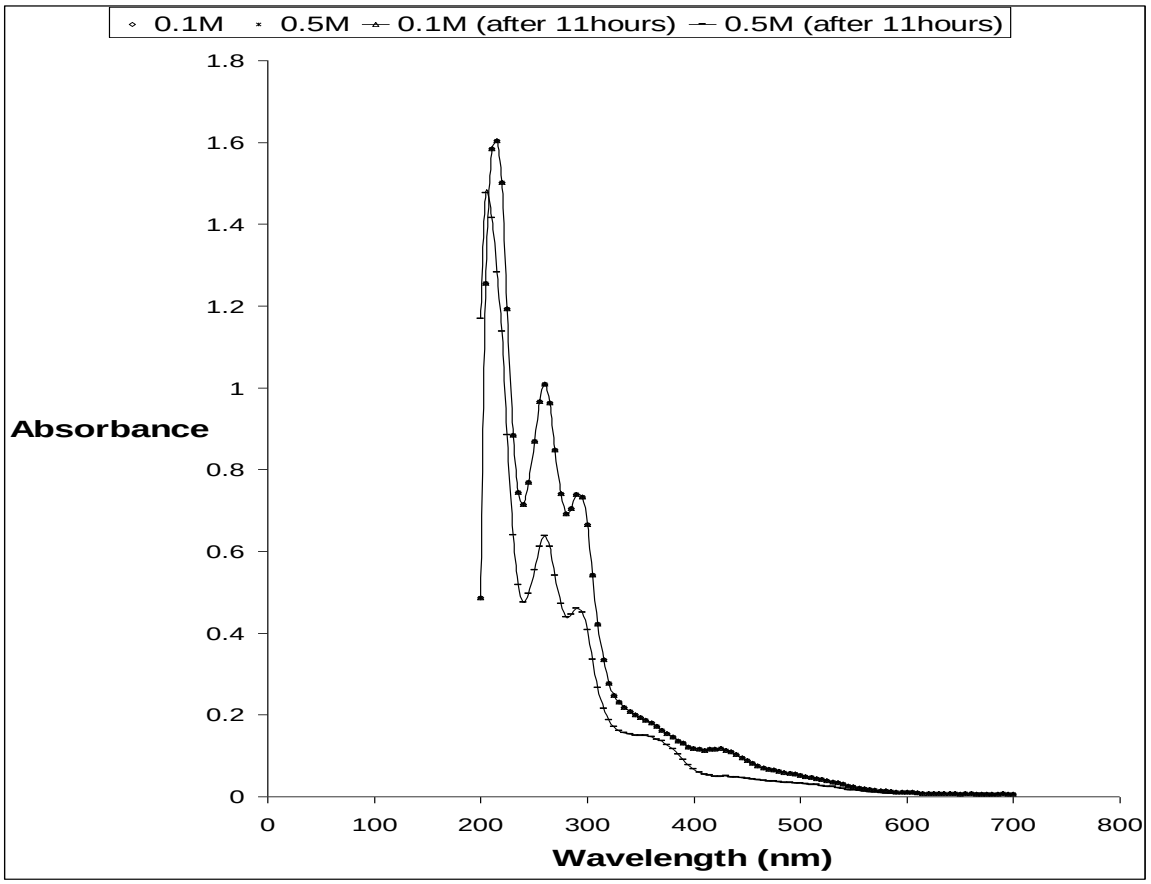

Figure 6. UV/visible spectra of ROST in 0.1M and 0.5M HCl solutions after 11 hours.

Figure 7 shows the variation in temperature with time for the dissolution of aluminum in 2.0 M HCl in the absence and presence of ROST. It can be observed from Figure 7 that the time required attaining the maximum temperature increases in the presence of ROST compared to the free acid. This behaviour reflects the high inhibition efficiency (%I) of the extracts which increase with increase in inhibitor concentration.

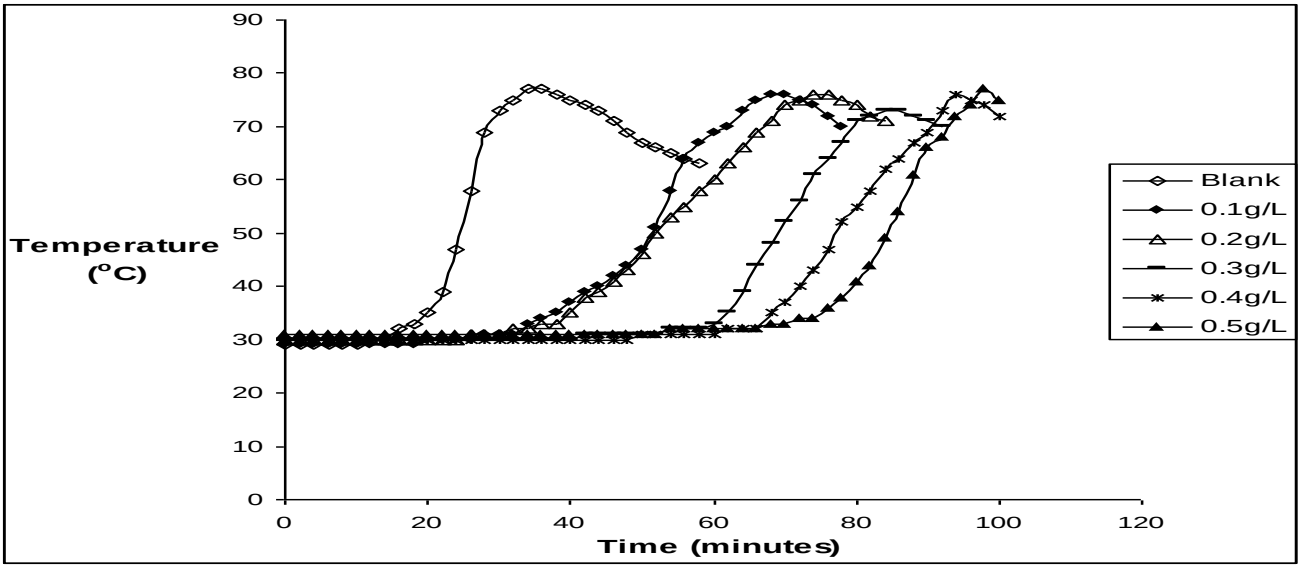

Figure 7. Variation of temperature with time for aluminium dissolution in 2.0 M HCl in the absence and presence of ROST.

3.3. Adsorption of ROST on aluminium

Organic inhibitors have been shown to act by adsorption on metal surfaces to inhibit metal corrosion [11, 16, 17]. The inhibitive effects of plant extracts have been attributed to the presence of chemical constituents (phytochemicals) [11]. Furthermore, it has been shown also [19] that organic inhibitors, tannins inclusive, possess some physico-chemical properties like: functional groups; aromaticity; steric effects; and electron density of donor atoms, which confer on them ability to adsorb on metal surfaces.

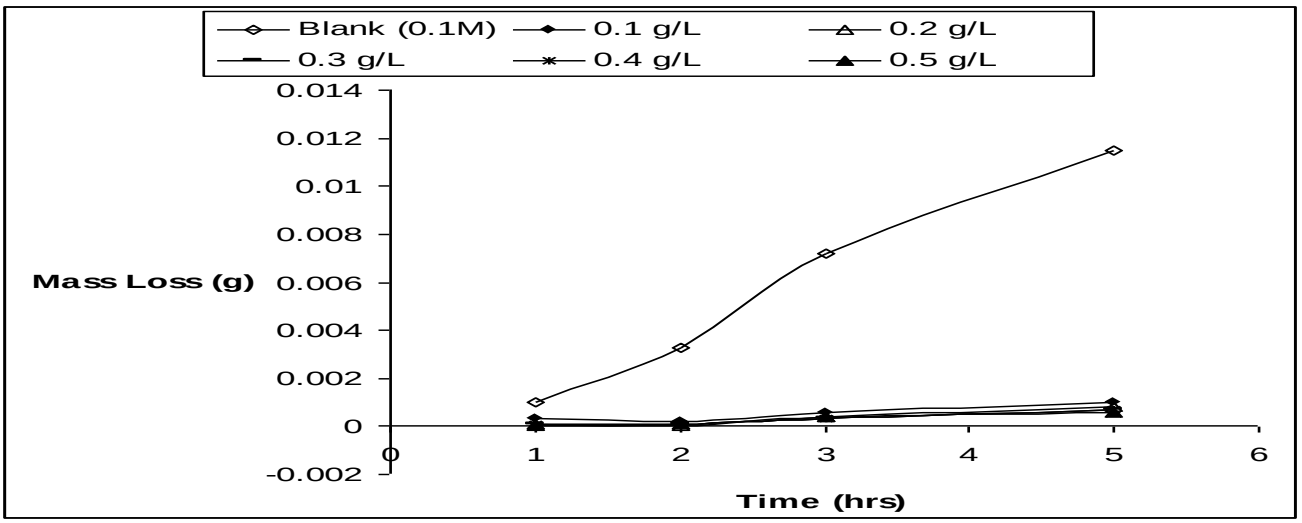

Figure 8. Variation of ROST mass loss with time in 0.1M hydrochloric acid at 30°C.

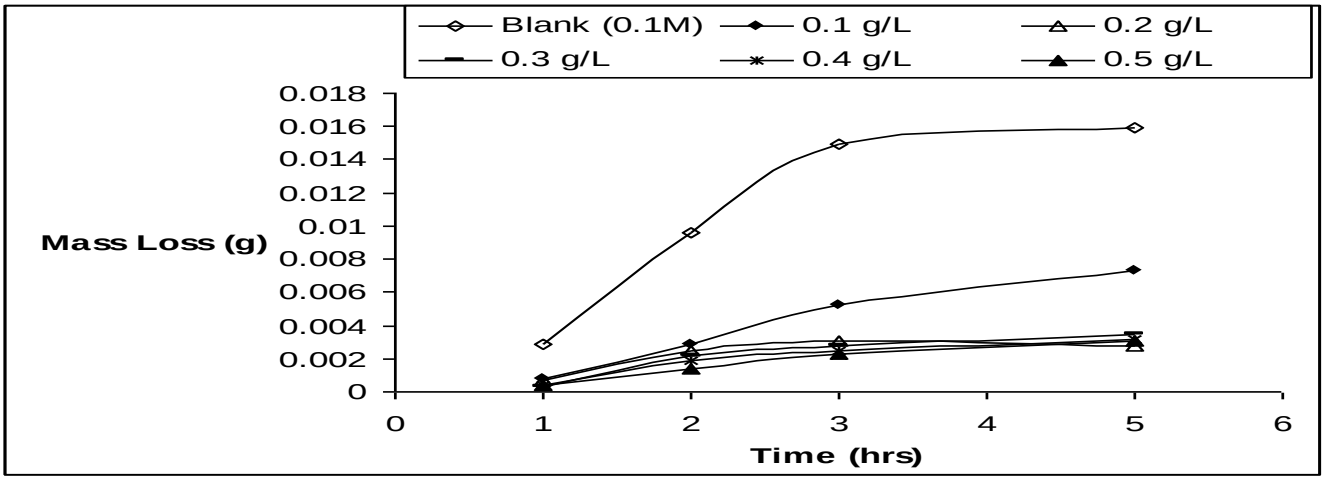

Figure 9. Variation of ROST mass loss with time in 0.1M hydrochloric acid at 40^{o}C.

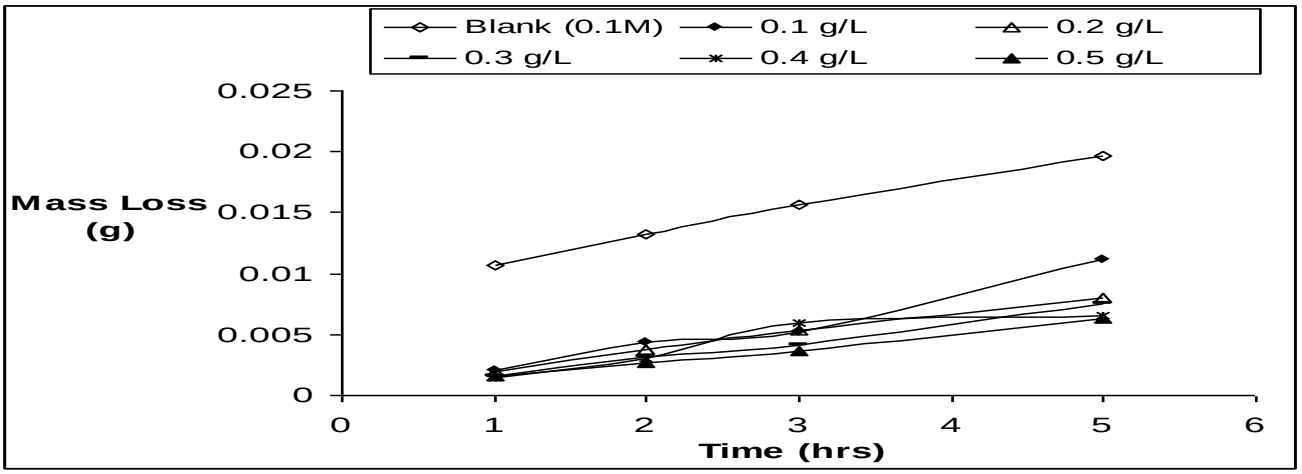

Figure 10. Variation of ROST mass loss with time in 0.1M hydrochloric acid at 50^{o}C.

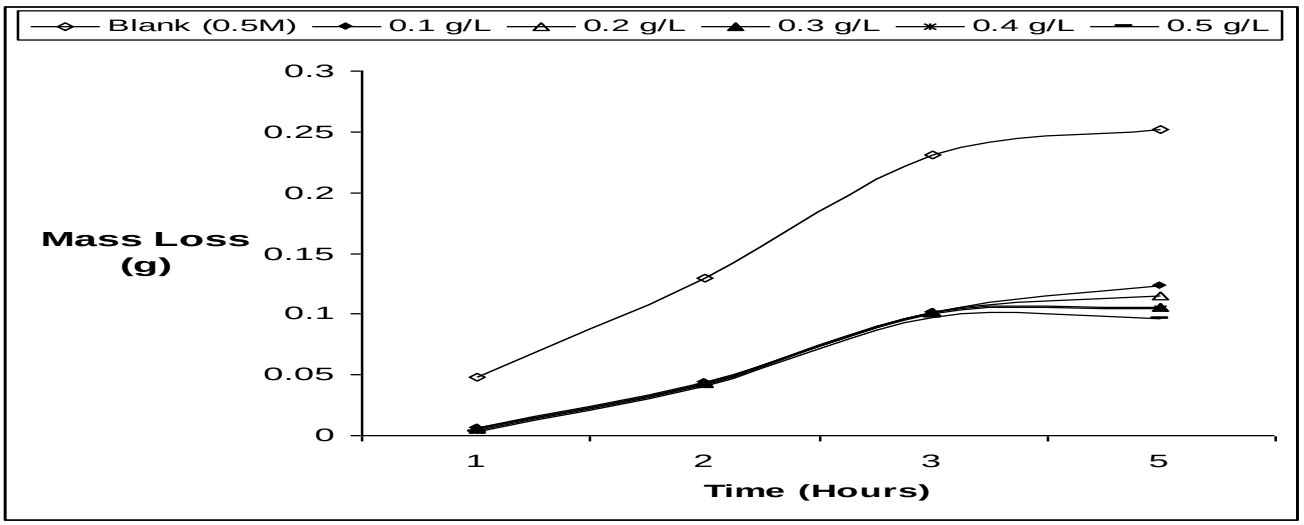

Figure 11. Variation of ROST mass loss with time in 0.5M hydrochloric acid at 30^{o}C.

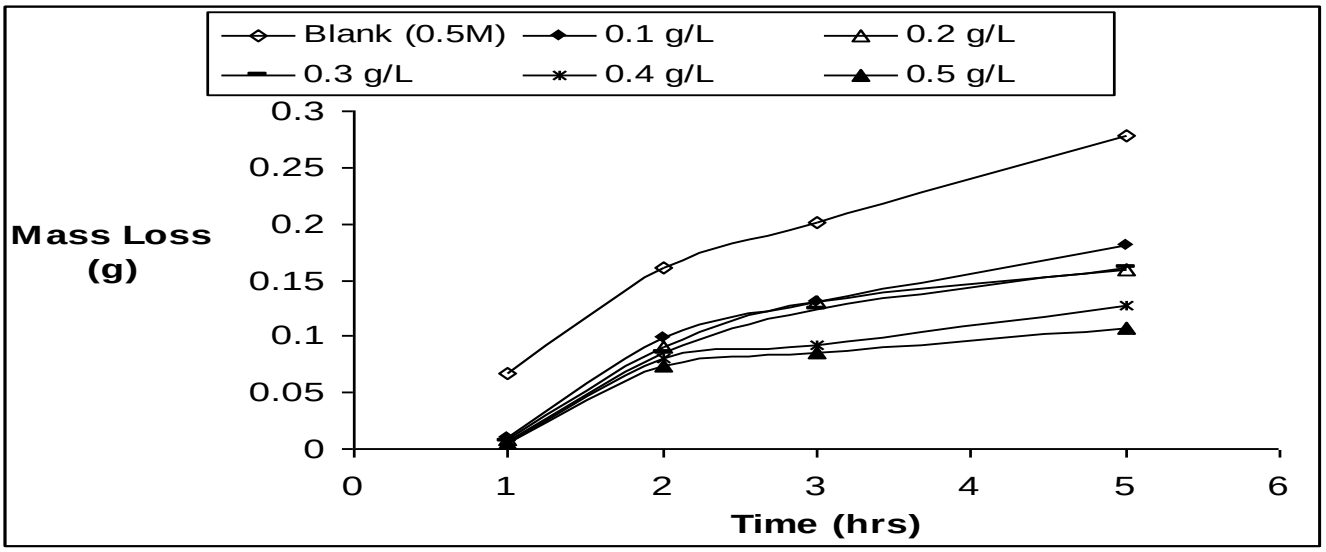

Figure 12. Variation of ROST mass loss with time in 0.5M hydrochloric acid at 40^{o}C.

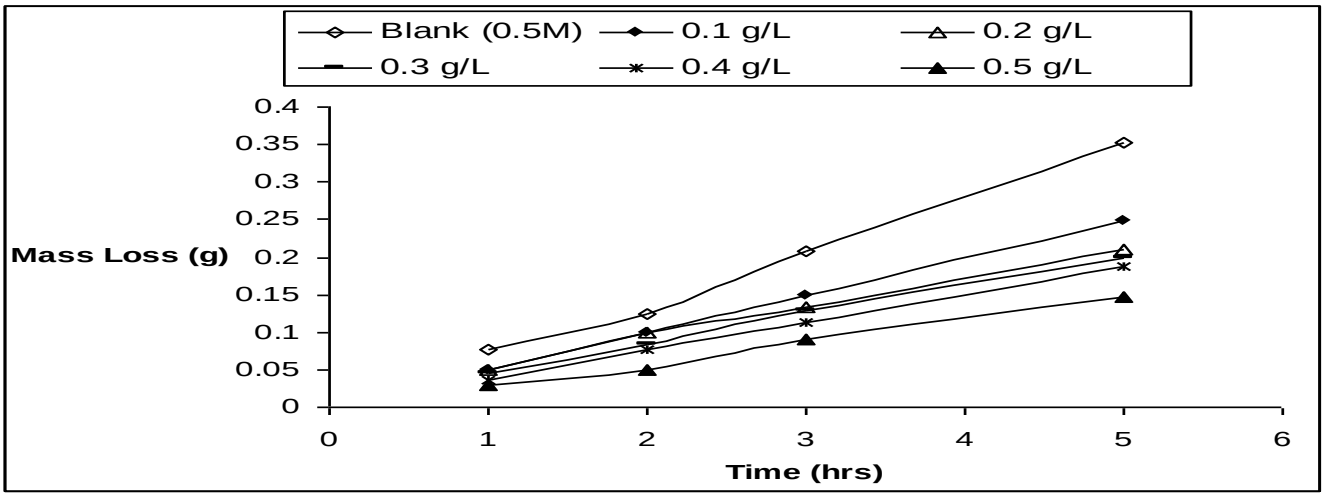

Figure 13. Variation of ROST mass loss with time in 0.5M hydrochloric acid at 50^{o}C.

Figures 4-6 show that ROST possess: aromatic centers and steric effects from flavonoid skeleton; and rich electron densities from oxygen atoms of the ketonic and phenolic functional groups of anthocyanins [13]. Therefore, ROST possesses required features for adsorption on aluminium.

The presence of ROST increased the longevity of aluminium in 0.1 M, 0.5 M and 2.0 M hydrochloric acid solutions as Figures 11-16 show. The dissolution of aluminium in 0.1 M, 0.5 M and 2.0 M hydrochloric acid solutions was fast but fortunately, Figures 8-13 also show that the presence of ROST in 0.1M and 0.5M hydrochloric acid solutions reduced the rate at which aluminium was attacked. The protection of aluminium in these hydrochloric acid solutions therefore is by adsorption of ROST on aluminium.

It is generally believed that aluminium becomes positively changed in aerated aqueous solutions. The characterization of ROST has shown it to be majorly made up of quercetin [13]. The structure of quercetin and its derivatives, as shown in Figure 3, show the presence of electron rich

centres like the aromatic ring, and oxygen atoms of polyphenols. The adsorption of ROST on aluminium is therefore believed to be enhanced by preventing a metal charge transfer, thereby reducing the rate at which aluminum was attacked. As evidenced by observed peak shift from 380 nm to 430 nm, shown in figure 3, adsorption on aluminium was via π-electron rich sites of ROST.

In order to elucidate the nature of adsorption of ROST, adsorption isotherm describing the adsorption process was determined. The commonest adsorption isotherms used are: Langmuir; Fruendlich; Temkin; and El-Awady models, respectively represented by the following expressions [11, 15- 19].

$$\theta = \frac{K_L C}{1 + K_L C} \tag{6}$$

$$\theta = K_F C^{\frac{1}{n}} \tag{7}$$

$$\ell^{f\theta} = K_T C \tag{8}$$

$$\theta = \frac{K_{EL} C^Y}{1 + K_{EL} C^Y} \tag{9}$$

where θ is the degree of surface coverage calculated from equation 3, adsorption capacity values determined from the different adsorption isotherms have the first letters of the authors who proposed them as subscripts- K_L, K_F, K_T and K_{EL}, $\frac{1}{n}$ and Y are adsorption constants from Fruendlich and El-Awady adsorption models which help to characterize the nature of inhibitor adsorption.

Equations 6-9 are non-linear and pose difficulty because of unavailability

of (special) programmes needed to handle them. Therefore, we resorted to the linearised versions of these non-linear equations which are respectively given below:

$$\frac{C}{\theta} = \frac{1}{K_L} + C \tag{10}$$

$$Ln\theta = LnK_F + \frac{1}{n} LnC \tag{11}$$

$$\theta = \frac{1}{f}\left(LnK_T + LnC\right) \tag{12}$$

$$Ln\left(\frac{\theta}{1-\theta}\right) = LnK_{EL} + YLnC \tag{13}$$

From equations 10-13, adsorption capacity values (K) were determined and presented in Table 1. Adsorption parameters from equations 10, 11 and 13 were substituted into equations 6, 7 and 9 to calculate theoretical surface coverage values (θ_{cal}). However, theoretical surface coverage values from Temkin isotherm were determined by substituting adsorption parameters from equation 12.

Table 1. Adsorption capacity (K_{ads}), standard free energy of adsorption (ΔG^{o}_{ads}), chi-square (χ^2) and surface coverage values of various linearised isotherms at 30ºC from gravimetric (0.1M) and (0.5M) and thermometric (2.0M) measurements.

Isotherm	Surface Coverage	System	Kads	ΔG^{o}_{ads} (KJ/mol)	χ^2
Langmuir – I	0.951, 0.975, 0.983, 0.987, 0.990	0.1M	192.308	-23.366	0.0072
(Hanes-Woolf]	0.796, 0.886, 0.921, 0.940, 0.951	0.5M	38.911	-19.341	0.4720
	0.523, 0.687, 0.767, 0.814, 0.846	2.0M	20.243	-17.694	0.3819
Temkin-I	0.914, 0.915, 0.916, 0.917, 0.918	0.1M	3.60×10^{14}	-268.568	0.0090
	0.571, 0.572, 0.574, 0.575, 0.576	0.5M	1.536×10^{19}	-121.409	0.0297
	0.875, 0.913, 0.935, 0.950, 0.962	2.0M	1.065×10^{8}	-56.688	2.4190
Freundlich-I	1.071, 1.078, 1.082, 1.085, 1.088	0.1M	1.095	-0.229	0.0089
	1.669, 1.693, 1.708, 1.718, 1.726	0.5M	1.752	-8.706	0.0271
	0.387, 0.411, 0.426, 0.437, 0.446	2.0M	0.474	-8.367	0.1286
El-Awady-I	0.106, 0.097, 0.093, 0.090, 0.087	0.1M	0.087	-6.151	0.0111
	0.318, 0.313, 0.310, 0.308, 0.307	0.5M	0.432	-2.114	0.0311
	0.329, 0.365, 0.387, 0.403, 0.416	0.835	0.835	-9.666	0.1317
Experiment	0.909, 0.944, 0.947, 0.947, 0.952	0.1M	---	---	---
	0.584, 0.600, 0.602, 0.617, 0.640	0.5M	---	---	---
	0.510, 0.560, 0.586, 0.603, 0.621	2.0M	---	---	---

Experimentally and theoretically determined surface coverage values were compared using chi-square statistic. The expression for chi-square statistic can be represented thus [20]:

$$\chi^2 = \Sigma \frac{(\theta_{\exp} - \theta_{cal})^2}{\theta_{cal}} \qquad (14)$$

where $\theta_{\exp}$ and θ_{cal} are experimental and theoretical/calculated surface coverage values respectively, and χ^2 is chi-square statistic. Values of calculated χ^2 are presented in Table 1 from which the lowest values give adsorption isotherm followed. From the calculated χ^2 values, it was concluded that Langmuir adsorption isotherm gave the best fit for data from 0.1 M HCl solutions and Fruendlich adsorption isotherm fitted well data from 0.5 M and 2.0 M HCl solutions.

Plot of equation 10, shown in Figure 14, using adsorption data for 0.1 M HCl solutions gave the following equation at 30°C:

$$y = 0.104x + 0.0052, R^2 = 1 \qquad (15)$$

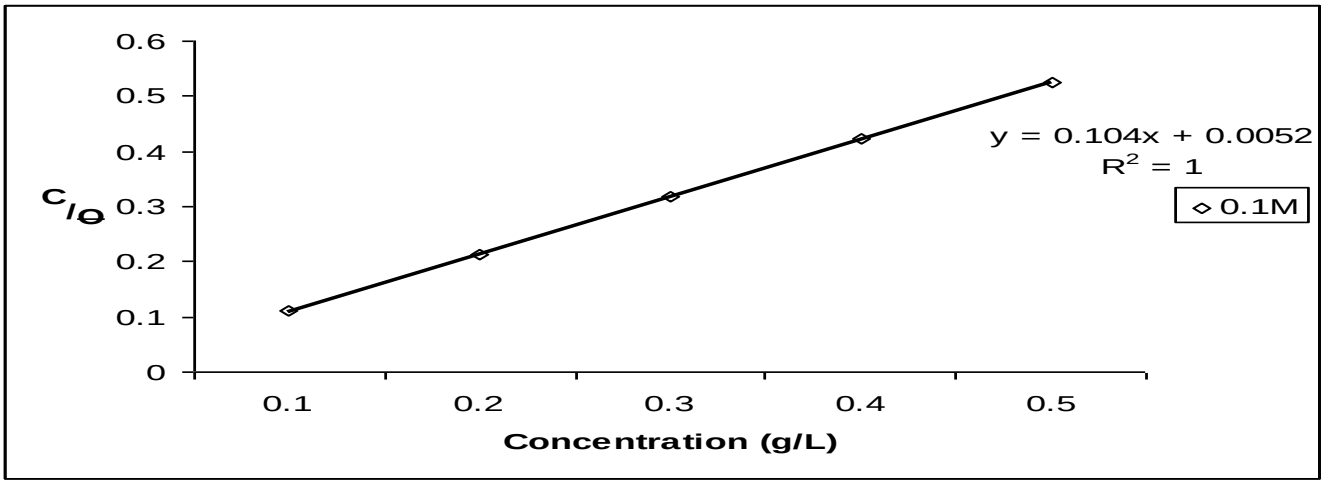

Figure 14. Langmuir plots for adsorption data in studied HCl solutions

Although coefficient of determination (R^2) has a value of unity, a slope of 0.104 deviates from the predicted value of unity from equation 17. This is suggestive of interactions of ROST molecules on aluminium such that high chemical adsorption or heavy physisorption must have occurred. Furthermore, it reveals therefore that the aluminium surface is characterized by non similar (heterogeneous) adsorption sites. These explanations were given because Langmuir [21] posited that surface adsorption sites are similar (homogeneous), therefore, adsorbing molecules would not interact with themselves, monolayer coverage by adsorbing molecules (chemisorption) is expected, and adsorption data would fit very well into equation 17.

For 0.5 M HCl solutions, adsorption data fitted equation 18, as shown in plot of Figure 15, at 30^{o}C from which the following equation was obtained:

$$y = 0.0212x - 0.5606, R^2 = 0.9414 \quad (16)$$

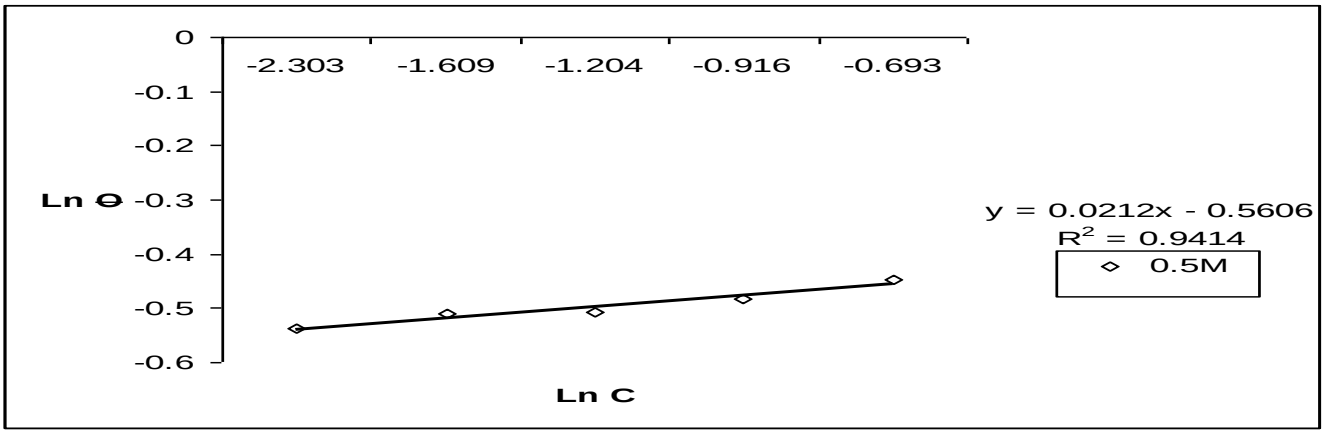

Figure 15. Fruendlich plot for adsorption data in studied 0.1 M HCl solutions

The coefficient of determination value is very high signifying well fitted adsorption data into Fruendlich isotherm. The intercept of -0.5606 was gotten which corresponds to LnK_F from which K_F value of 0.571 was calculated. The K_F value denotes the strength between adsorbate and adsorbent such that small K_F value implies physisorption [22]. The slope of 0.0212 from equation 18 corresponds to $\frac{1}{n}$ of equation 14, its small value no doubts, indicates physisorption.

In the same vein for 2.0 M HCl solutions, adsorption data fitted equation 18, as shown in plot of Figure 16, at 30^{o}C from which the following equation was obtained:

$$y = 0.0468x - 0.6942, R^2 = 0.9271 \quad (17)$$

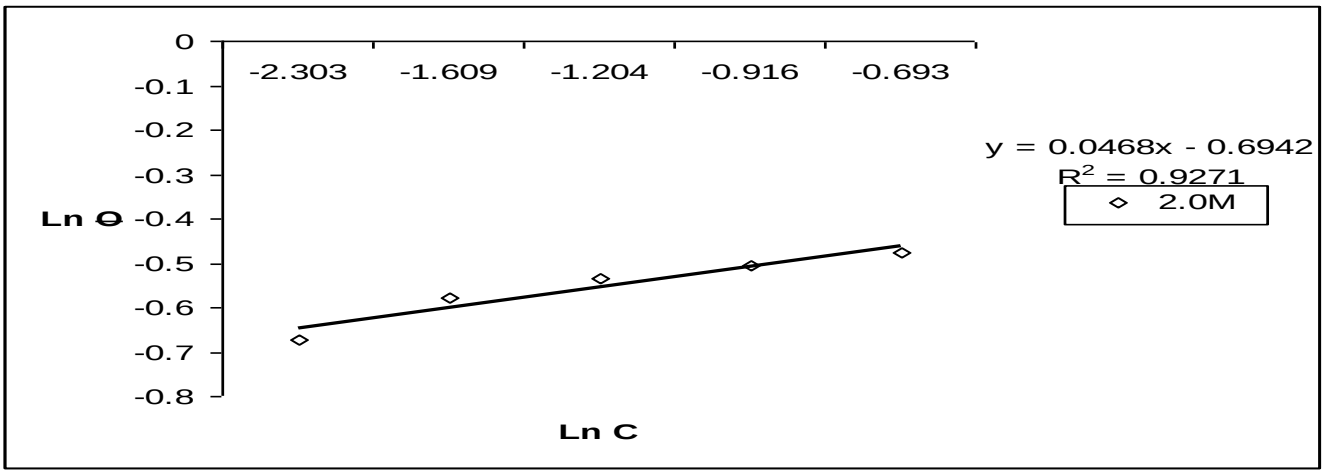

Figure 16. Fruendlich plot for adsorption data in studied 0.1 M HCl solutions

The coefficient of determination value is also very high signifying well fitted adsorption data into Fruendlich isotherm. The intercept of -0.6942 was gotten which corresponds to LnK_F from which K_F value of 0.499 was calculated. The K_F value denotes the strength between adsorbate and adsorbent such that small KF value implies physisorption [23]. The slope of 0.0468 from equation 18 corresponds to $\frac{1}{n}$ of equation 14, its small value no doubts, indicates physisorption.

3.4 Thermodynamics of ROST adsorption on aluminium in HCl

Thermodynamic model is an important tool to study the mechanism of inhibition on the corrosion of metals [17, 22], therefore, a thermodynamic model was chosen/selected so that complete understanding of the ROST inhibition mechanism on aluminium corrosion would be possible.

Free energy of adsorption for ROST adsorption on aluminum was obtained using the following expression [15-17]:

$$K_{ads} = \frac{1}{55.5} \ell^{-\frac{\Delta G}{RT}} \quad (18)$$

where K_{ads} is the adsorption capacity, R is the gas constant and T is temperature in Kelvin. The free energy of adsorption, ΔG_{ads}, which can characterize the interaction of ROST on metal surface [19], was calculated and presented in Table 1. The negative values of ΔG_{ads} ensure the spontaneity of adsorption process and stability of the adsorbed layer on the aluminium surface [18]. Usually, the values of ΔG_{ads} around -20 kJ/mol (and lower magnitude) are consistent with physisorption and those around -40 kJ/mol (and higher magnitude) involve chemisorption [16]. The of ΔG_{ads} shown in Table 1 for 0.1 M HCl is -23.366 kJ/mol, hence, suggests physisorption of ROST on aluminium in 0.1 M HCl. From Table 1 also, free energy values of -8.706 and -8.367 for 0.5M and 2.0M HCl solutions containing ROST respectively, indicate physisorption.

The well known thermodynamic adsorption parameters- free energy of adsorption (ΔG_{ads}), heat of adsorption (ΔH_{ads}) and entropy of adsorption (ΔS_{ads}), were determined. The values of ΔG_{ads} calculated were done using equation 18 and presented in Table 1. Calculated ΔG_{ads} values were plotted against temperature (T), in Figure 20, with a thermodynamic expression as shown below:

$$\Delta G_{ads} = \Delta H_{ads} - T\Delta S_{ads} \quad (19)$$

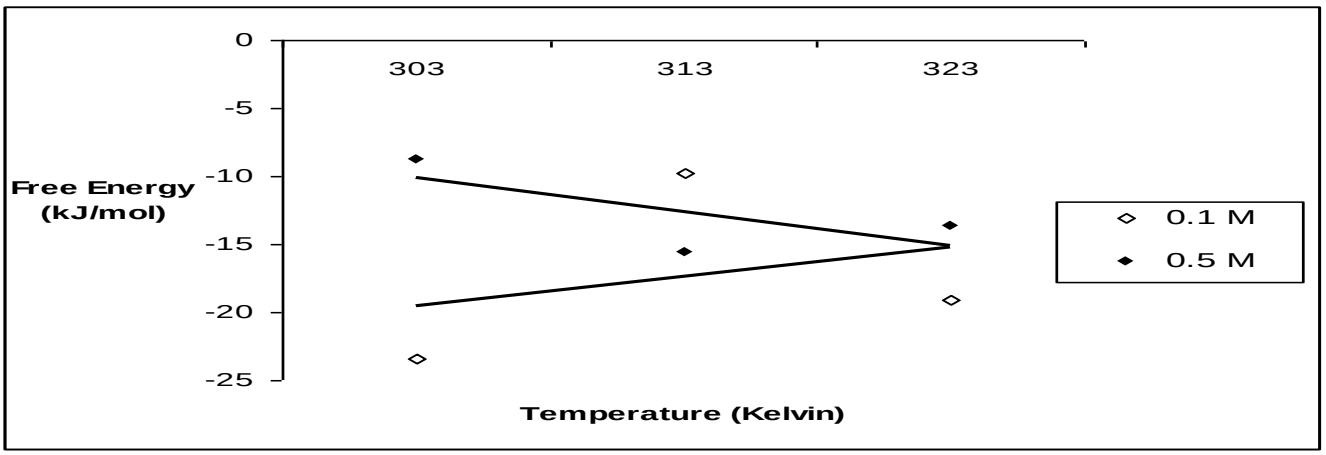

Figure 20. Plots of ΔG_{ads} against T

Table 2. Thermodynamic parameters for ROST adsorption on aluminium in 0.1 M and 0.5 M HCl solutions

System	**ΔG_{ads} ($kJmol^{-1}$)**	**ΔH_{ads} ($kJmol^{-1}$)**	**ΔS_{ads} ($kJmol^{-1}$)**	**Temperature**
0.1 M	-23.367	-21.659	0.0056	30^{o}C
	-09.734	-21.659	-0.0381	40^{o}C
	-19.113	-21.659	-0.0079	50^{o}C
0.5 M	-08.706	-07.663	0.0034	30^{o}C
	-15.533	-07.663	0.0251	40^{o}C
	-13.684	-07.663	0.0192	50^{o}C

On careful observation, one identifies that equation 19 is similar to a straight line equation such that the intercepts gotten from the plots represent ΔH_{ads}. The values of ΔH_{ads} thus obtained were introduced into equation 26 therefore allowing the calculations of ΔS_{ads}. Calculated thermodynamic parameters are presented in Table 2.

Calculated negative values of ΔG_{ads} indicating that ROST adsorption on aluminium in HCl solutions are spontaneous. In addition, ΔH_{ads} values are negative suggestive of exothermic adsorption processes by ROST on aluminium in HCl solutions. From values of ΔH_{ads} in Table 2 which are not up to -40 $kTmol^{-1}$, ROST adsorption processes on aluminium in HCl solutions are indicative of physical adsorption.

3.5. Effect of temperature on ROST adsorption

The effect of temperature on ROST adsorption on aluminum in hydrochloric acid solutions was studied. Usually, the Arrhenius plots of equation 20 come handy in thermodynamic modeling [22]. Calculated corrosion rates (C_{corr}) of aluminium in 0.1M and 0.5M HCl solutions at 30°C-50°C were used to make the Arrhenius plots. The values of frequency factor (A) and activation energy (E_a) were determined from Arrhenius plots of equation 20.

$$LnC_{corr} = LnA - \frac{E_a}{T} \quad (20)$$

Respectively, A and E_a were gotten from intercepts and slopes of equation 20 plots and presented in Tables 3 and 4. Tables 3 and 4 show that in 0.1M HCl and 0.5M HCl solutions, A values for aluminium dissolution are higher in blank solutions than in solutions containing various concentrations of ROST. These are evidence of good inhibition efficiency exhibited by ROST [11]. Activation energy values obtained from slopes of equation 20 plots for 0.1M and 0.5M HCl blanks are lower than values obtained for systems containing ROST. This also confirms what was observed in the laboratory that the presence of ROST, prolonged the longevity of aluminium 0.1M and 0.5M HCl solutions.

Table 3: Calculated values for activation energy (E_a) and frequency factor (A) of 0.1M system

System	A x 10^{-4}	E_a (J/mol)
Blank Inhibitor ($^g/_L$)	4.545	0.472
0.1	3.874	1.197
0.2	4.076	1.345
0.3	3.417	1.301
0.4	3.507	1.322
0.5	2.864	1.283

Table 4: Calculated values for activation energy (E_a) and frequency factor (A) of 0.5M system

System	A x 10^{-4}	E_a (J/mol)
Blank Inhibitor ($^g/_L$)	3.702	0.070
0.1	3.134	0.343
0.2	2.729	0.310
0.3	2.362	0.276
0.4	1.647	0.247
0.5	3.593	0.141

3.6. Kinetics of ROST adsorption

A work [16] suggests that adsorption of corrosion inhibitors obey a kinetic relationship represented thus:

$$LnC_{corr} = LnK + BLnC_{inh} \quad (21)$$

where K is the rate constant, B is the reaction constant and C_{inh} is the inhibitor concentration in g/L. Linear plots were done and determined kinetic parameters are shown in Table 5.

Table 5. Kinetic parameters for ROST adsorption

System	Reaction Constant (B)			Rate Constant (K) × 10^{-3}		
	30°C	40ºC	50°C	30ºC	40ºC	50ºC
0.1M	-0.483	-0.348	-0.283	0.0532	0.158	0.250
0.5M	-0.197	-0.188	-0.139	2.601	3.310	3.604

Negative values of reaction constant were obtained and are indicative that increase in inhibitor concentration decreases corrosion inhibition [15, 16]. It can be observed from Table 5 that rate constants from equation 21 plots and frequency factor values from Arrhenius plots of equation 20 are of the same order. These strengthen the fact that ROST adsorption on aluminium can be accounted for by the kinetic expression of equation 21.

The major reaction that explains aluminium corrosion in hydrochloric acid can be represented as

$$2Al_{(s)} + 6HCl_{(aq)} \rightarrow 2AlCl_{3(aq)} + 3H_{2(g)} \quad (22)$$

In the absence of ROST, but in the presence of air and moisture, formation of oxide films has been reported. These oxide films (Al_2O_3, $Al(OH)_3$ and AlO.OH) have been reported to decrease the rate at which aluminum corrodes [23]. Reaction pathways that account for the formation of these aluminum compounds can be represented thus

$$4Al_{(s)} + 30_{2(g)} \rightarrow 2Al_2O_{3(s)} \quad (23)$$

$$2Al_{(s)} + 6H_2O_{(l)} \rightarrow 2Al(OH)_{3(s)} + 3H_{2(g)} \quad (24)$$

$$2Al_{(s)} + 4H_2O_{(l)} \rightarrow 2AlO.OH_{(s)} + 3H_{2(g)} \quad (25)$$

Regrettably, the presence of anions such as Cl^- breakdown the passivity of aluminium, therefore, the protection aluminium enjoys fails. The addition of corrosion inhibition becomes vital for continued aluminium protection.

The presence of ROST therefore brings about the production of other corrosion products, hence, the chemistry of this process can be presented as

$$Al + ROST \leftrightarrow [Al.ROST] \rightarrow products \quad (26)$$

It is clear that for the corrosion inhibition process, equations 23-26 occur, therefore, the corrosion inhibition process is a complex reaction type. To account for these reactions we propose that parallel reactions occur such that equation 23 is the main reaction in the corrosion process. The side reactions involve equations 23-25 for corrosion process without ROST and equations 23-26 for corrosion process with ROST present.

A general expression representing the parallel reactions therefore is

$$Al_{(s)} + HCl_{(aq)} \xrightarrow{k_1} AlCl_{3(aq)} + H_{2(g)} \quad (27)$$

$$Al_{(s)} + Inh \overset{K_c}{\leftrightarrow} [Al.Inh] \overset{k_2}{\rightarrow} products \quad (28)$$

where [Al.Inh] represents Al_2O_3, $Al(OH)_3$ and AlO.OH in the absence of ROST and [Al.ROST] in the presence of ROST. k_1 rate constant for the dissolution of aluminium, k_2 is the unimolecular rate constant for decomposition of activated complex, and K_c the proportionality constant for the formation of activated complex. Values of calculated k, k_1, k_2, and K_C are presented in Tables 6 and 7.

Table 6. Bimolecular or overall rate constant (k), proportionality constant (K_C), unimolecular rate constant (k_2), change in number of moles of evolved hydrogen gas (Δn), and free energy of adsorption and other kinetic parameters for 0.1M system at 30°C.

System	k x 10^{12}	K_c	k_2 x 10^{12}	Δn	ΔG (KJ/mol)
Bland Inhibitor ($^g/_L$)	5.868	0.9642	6.081010	-0.000106	1.746
0.1	5.858	0.9634	6.081010	-0.000106	1.773
0.2	5.859	0.9634	6.081319	-0.000107	1.768
0.3	5.856	0.9632	6.080247	-0.000107	1.790
0.4	5.857	0.9633	6.080404	-0.000106	1.787
0.5	5.855	0.9631	6.079173	-0.003875	1.577

Table 7. Bimolecular or overall rate constant (k), proportionality constant (K_C), unimolecular rate constant (k_2), change in number of moles of evolved hydrogen gas (Δn), and free energy of adsorption and other kinetic parameters for 0.5M system at 30°C.

System	k x 10^{12}	K_c	k_2 x 10^{12}	Δn (KJ/mol)	ΔG
Bland Inhibitor ($^g/_L$)	5.884	0.9655	6.094758	-0.000104	1.472
0.1	5.884	0.9655	6.094572	-0.000104	1.479
0.2	5.883	0.9654	6.093740	-0.000105	1.496
0.3	5.881	0.9652	6.092896	-0.000106	1.513
0.4	5.879	0.9651	6.092018	-0.000105	1.532
0.5	5.880	0.9651	6.092219	0.003669	1.811

Considering rate measurements from gravimetry, the reaction rate constant, k_1, can be determined from the differential rate law

$$\text{Corrosion Rate} = \frac{-d[Al]}{dt} = k_1[Al] \quad (29)$$

Rearranging equation 29 gives

$$\int_{[Al_0]}^{[Al]} \frac{d[Al]}{[Al]} = -k_1 \int_o^t dt \quad (30)$$

Solving equation 30 gives

$$\text{In}\left(\frac{[Al]_o}{[Al]}\right) = k_1 t \quad (31)$$

where $[Al]_o$ is the weight of aluminium coupon before corrosion, [Al] is the weight of aluminium at different time intervals during corrosion, t is the time involved. Plots of equation 31 suggest first order kinetics. From the slopes of these plots, k_1 can be calculated. Substituting k_1 values into equation 32, enables the determinations of half-lives ($t_{\frac{1}{2}}$) for the various corrosion processes.

$$t_{1/2} = \frac{0.693}{k_1} \quad (32)$$

Half-life values are presented in tables 8 and 9 and reveal that the presence of ROST extended the duration of the corrosion of aluminium in 0.1M and 0.5M HCl solutions at studied temperatures. However, lower values of half-life for 0.5M HCl suggest that aluminium was better protected by ROST, in 0.1M HCl.

Table 8. Half-lives ($t\frac{1}{2}$) in days for 0.1M HCl Solutions.

System	30°C	40°C	50°C
Bland Inhibitor ($^{g}/_{L}$)	154.000	79.655	73.723
0.1	1,732.500	2,310.000	173.250
0.2	3,465.000	407.647	31.789
0.3	3,465.000	385.000	238.966
0.4	3,465.000	462.000	231.000
0.5	3,465.000	495.000	277.200

In chemistry, reactions are thought to progress when reactants possess enough energy (activation energy) to react and form products. Consequently, these reactants acquire energy to form an activated complex which then decomposes into products. This can be illustrated thus:

$$\mathrm{Re}actants \leftrightarrow ActivatedComplex \rightarrow \mathrm{Pr}oducts \quad (33)$$

From the foregoing, the aluminium corrosion inhibition by ROST can therefore be represented by equation 33. From equation 33, an overall rate for the corrosion process can be written as given below

$$Rate = k[Al][ROST] \quad (34)$$

Table 9: Half-lives ($t\frac{1}{2}$) in days for 0.5M HCl Solutions.

System	30°C	40°C	50°C
Bland Inhibitor ($^{g}/_{L}$)	4.679	4.213	3.572
0.1	11.826	7.444	5.964
0.2	12.623	7.822	7.166
0.3	12.509	8.566	7.166
0.4	13.200	10.043	8.299
0.5	13.562	12.739	11.455

where k is the overall rate constant for the dissolution of aluminium. A rate equation for the production of activated complex can be expressed mathematically assuming that the reactants are in equilibrium with the activated complex (as shown in equation 33).

$$k_{C_1}[Al][ROST] = k_{C_{-1}}[Al.ROST] \quad (35)$$

Rearranging equation 35 gives equations 36 and 37 thus

$$[\mathrm{Al.ROST}] = \frac{k_{C_1}}{k_{C_{-1}}}[Al][ROST] \quad (36)$$

$$= K_c[\mathrm{Al}][\mathrm{ROST}] \quad (37)$$

Comparing equations 36 and 37 reveals that $K_c = \frac{k_{C_1}}{k_{C_{-1}}}$, hence its name, proportionality constant.

From the unimolecular decomposition of the activated complex shown by equation 33, another rate equation can be written as

$$rate = k_2[Al.ROST] \quad (38)$$

Substituting the expression for [Al.ROST] given by equation 38, equation 38 becomes

$$rate = k_2 K_C[Al][ROST] \quad (39)$$

Close observation of equation 33 clearly shows that the corrosion process goes through two major steps: formation of activated complex and decomposition of activated complex. These two major gave rise to expressions 34 and 38. Therefore, equating the overall rate equation represented by equation 34 and equation 38 which represents the corrosion steps, the following equation was obtained

$$Rate = k[Al][ROST] = k_1 K_C[Al][ROST] \quad (40)$$

This obviously makes the overall rate constant, k, be related thus

$$k = k_1 K_C \quad (41)$$

The overall rate constant is also known as the bimolecular rate constant for the corrosion inhibition process involving reaction between aluminium and ROST. The proportionality constant (K_C) has relationship with the unimolecular rate constant (k_1) thus [24]:

$$k_1 = \frac{RT}{Nh} K_C \quad (42)$$

The proportionality constant has been shown to have the following expression [24, 25]

$$K_C = \ell^{\frac{-\Delta G}{RT}} \quad (43)$$

Equation 43 was used to calculate K_C values. Substituting K_C values into equation 40, k_1 values were calculated. The values of k were also calculated from equation 40 after substituting values for k_1 and K_C. The calculated values of k, k_1, and K_C for 0.1M and 0.5M HCl solutions are presented in Tables 10 and 11.

It is well known that higher values of rate constant implies faster rate of reaction. From equation 38 therefore, it is expected that corrosion rate increase when k_2 increase. Thus higher k_2 values, presented in tables 10 and 11, for blanks are more than those containing ROST, hence, reveal more aluminium corrosion than systems containing ROST which have lower k_2 values. 0.5M HCl solutions have higher k_2 values than 0.1M HCl solutions, implying that more aluminium corrosion took place in 0.5M HCl solutions. Also from equations 27 and 31, it is expected that higher k_1 values would support more aluminium corrosion. Determined k_1 values for systems containing ROST in 0.1M and 0.5M HCl solutions are lower than blanks, therefore depict aluminium corrosion inhibition in 0.1M and 0.5M HCl solutions.

A close observation of equations 31 and 32 reveals that hydrogen is given off during aluminium corrosion in HCl. Assuming ideal gas behaviour for the hydrogen gas evolved, equation 44 gives a relationship between heat of ROST adsorption on aluminium and energy of activation in HCl solutions [24].

$$\Delta H = E_a + \Delta n(RT) \quad (44)$$

where Δn is the number of moles of hydrogen gas evolved. Expected too is that more negative Δn value should favour better corrosion inhibition whereas more positive values should favour aluminium corrosion. However from Tables 10 and 11, Δn values for 0.5 M HCl solutions are more positive than for 0.1M HCl solutions, therefore suggests that aluminium corroded more in 0.5 M HCl solution.

4. CONCLUSION

The following salient points highlight the conclusion of this work:

- ROST inhibits aluminium corrosion in 0.1M and 0.5M hydrochloric acid solutions effectively;
- Corrosion inhibition of ROST increases as inhibitor concentration increases;
- Increasing the concentration of hydrochloric acid decreases the inhibition efficiency of ROST;
- Langmuir adsorption isotherm gives the best fit for obtained adsorption data in 0.1M HCl solutions, and Fruendlich adsorption isotherm for adsorption data in 0.5M and 2.0M HCl solutions;
- Determination of free energy of adsorption of ROST on aluminium was from obtained adsorption parameters and gave values characteristic of physisorption;
- Thermodynamics studies reveal effective inhibition of aluminium corrosion in hydrochloric acid solutions by ROST. Inaddition, temperature variation studies further reveal that inhibition efficiency of ROST decreases as temperature increases. This is characteristic of physisorption;
- Adsorption physical adsorption (physisorption) mechanism by ROST adsorption on aluminium in hydrochloric acid solutions.

References

1. P.O. Ukoha, E.N. Oparah, and C.C. Maju, *J. Chem. Soc. Nig.*, 30 (1) (2005) 53
2. P.O. Ukoha, P.M Ejikeme and C.C. Maju, *J. Am. Lea. Chem. Assos.*, 106 (2010) 247
3. I.L. Finar, *Organic Chemistry Volume 2: Stereo chemistry and the Chemistry of Natural Products-5th edition*, India:Eastern Priest, Bemgalone (2000)
4. O.A. Sodipo, F.I. Abdulrahman, J.C. Akan, and J.A. Akinniyi, *Continental J. Appl. Sci.*, 3 (2008) 85
5. S.Y. Wang, Y.H. Kuo, H.N. Chang, P.L. Kang, H.S. Tsay, K.F. Lin, N.S. Yang, and L.F. Shyer, *J. Agric. Food Chem.*, 50 (2002) 1859
6. S.D. Karou, W.M.C. Nadembega, P.D. IIboudo, D. Ouermi, M. Gbeassor, C. De Souza, and J. Simpore, *Afr. J. Biotech.*, 6 (25) (2007) 2953
7. Y.L. Qing, J.R. Arteaga, Q. Zhang, S. Huerta, V.L.W. Go, and D. Heber, *J. Nut Biochem.*, 16 (2005) 23
8. J.J.G Leite, E.H.S. Brito, R.A. Cordeiro, R.S.N. Brilhante, J.J.C. Sidrim, L.M. Bertini, S.M. de Morais, and M.F.G. Rocha, *Acta Tropical*, 42 (2) (2009) 111

9. O. Krishnaiah, T. Devi, A. Bono, and R. Sarbatly, *J. Med. Plants Res.*, 3 (2) (2009) 69
10. G.N. Anyasor, D.A. Aina, M. Olushola, and A.F. Aniyikaye, *Anal. Bio. Res.*, 2 (2) (2011) 448
11. S.A. Umoren, O. Ogbobe, E.E. Ebenso, *Transactions of the SAEST* 41 (2006) 74
12. B.S. Furniss, A.J. Hannaford, P.W.G. Smith, and A.R. Tatchell, *Vogel's Textbook of Practical Organic Chemistry-5th Edition*, Longman Group, Essex (1989)
13. K. Nemeth, and M.K. Piskula, *Crit. Rev. Food Sci. Nut.*, 47 (4) (2007)397
14. M. Guisti, and R.E. Wrolstad, *Current Protocols in Food Analytical Chemistry*, John Wiley & Sons Inc., New York (2001)
15. N.O. Obi-Egbedi, K.E. Essien, and I.B. Obot, *J. Comput. Method Mol. Design*, 1 (1) (2011) 26
16. E.A. Noor, *Int. J. Electrochem. Sci.*, 2 (2007) 996
17. S.A. Abd El-Maksoud, *Int. J. Electrochem. Sci.*, 3 (2008) 528
18. P.C. Okafor, U.J. Ekpe, E.E. Ebenso, E.E. Oguzie, N.S. Umo, and Etor, *Transactions of the SAEST* , 41 (2006) 82
19. I.B. Obot, N.O. Obi-Egbedi, and S.A. Umoren, *Int. J. Electrochem. Sci.*, 4 (2009) 863
20. B.G. Nworgu, *Educational Research- Basic Issues and Methodology*, University Trust Publishers, Nsukka (2006)
21. I. Langmuir, *J. Am. Chem. Soc.*, 38 (1916) 2221
22. N.J.N. Nnaji, N.O. Obi-Egbedi, and J.U. Ani, *Int. J. Chem.*, 3 (2011)19
23. A.K. Mishra, R. Balasubramaniam, *Mater. Chem. & Phy.*, 103 (2007) 358
24. K.K Sharma, L.K. Sharma, *A Textbook of Physical Chemistry-4th revised edition*, Vikas Publishing House PVT Ltd., New Delhi (1999)
25. E.C. Okafor, *Physical Chemistry-Fundamentals*, Snaap Press Ltd., Enugu (2004)